CrossMark

REGULAR ARTICLE

Expression studies of neuronatin in prenatal and postnatal rat pituitary

Naoko Kanno[1] · Masashi Higuchi[2,3] · Saishu Yoshida[1] · Hideji Yako[1] · Mo Chen[2,3] ·
Hiroki Ueharu[1] · Naoto Nishimura[1] · Takako Kato[2,3] · Yukio Kato[1,3]

Abstract The pituitary gland, an indispensable endocrine organ that synthesizes and secretes pituitary hormones, develops with the support of many factors. Among them, neuronatin (NNAT), which was discovered in the neonatal mouse brain as a factor involved in neural development, has subsequently been revealed to be coded by an abundantly expressing gene in the pituitary gland but its role remains elusive. We analyze the expression profile of *Nnat* and the localization of its product during rat pituitary development. The level of *Nnat* expression was high during the embryonic period but remarkably decreased after birth. Immunohistochemistry demonstrated that NNAT appeared in the SOX2-positive stem/progenitor cells in the developing pituitary primordium on rat embryonic day 11.5 (E11.5) and later in the majority of SOX2/PROP1 double-positive cells on E13.5. Thereafter, during pituitary embryonic development, *Nnat* expression was observed in some stem/progenitor cells, proliferating cells and terminally differentiating cells. In postnatal pituitaries, NNAT-positive cells decreased in number, with most coexpressing *Sox2* or *Pit1*, suggesting a similar role for NNAT to that during the embryonic period. NNAT was widely localized in mitochondria, peroxisomes and lysosomes, in addition to the endoplasmic reticulum but not in the Golgi. The present study thus demonstrated the variability in expression of NNAT-positive cells in rat embryonic and postnatal pituitaries and the intracellular localization of NNAT. Further investigations to obtain functional evidence for NNAT are a prerequisite.

Keywords Neuronatin · Rat pituitary · Stem/progenitor cells · SOX2 · PROP1

✉ Yukio Kato
yukato@meiji.ac.jp

1 Division of Life Science, Graduate School of Agriculture, Meiji University, Kanagawa 214-8571, Japan

2 Organization for the Strategic Coordination of Research and Intellectual Property, Meiji University, Kanagawa 214-8571, Japan

3 Institute of Reproduction and Endocrinology, Meiji University, Kanagawa 214-8571, Japan

Abbreviations

ACTH	Adrenocorticotropic hormone
DAPI	4′ 6-Diamidino-2-phenylindole
ER	Endoplasmic reticulum
EYFP	Enhanced yellow fluorescent protein
FITC	Fluorescein isothiocyanate
FSHβ	Follicle-stimulating hormone
GFP	Green fluorescent protein
GH	Growth hormone
LHβ	Luteinizing hormone
MCL	Marginal cell layer
NNAT	Neuronatin
PCR	Polymerase chain reaction
PDI	Protein disulfide isomerase
PIT1	Pituitary-specific transcription factor 1
PRL	Prolactin
PROP1	Prophet of PIT1
PRRX1	Paired-related homeobox 1
PRRX2	Paired-related homeobox 2
SERCA2	Sarco/endoplasmic reticulum Ca^{2+} ATPase isoform 2
SOX2	Sex-determining region Y-box 2

| TBP | TATA-box-binding protein |
| TSHβ | Thyroid-stimulating hormone |

Introduction

The pituitary gland is composed of the adenohypophysis (anterior and intermediate lobes) and neurohypophysis (posterior lobe) and plays essential roles in growth, metabolism, reproduction, lactation, homeostasis and the stress response by secreting pituitary hormones. Hormone-producing cells in the anterior and intermediate lobes differentiate during embryonic organogenesis under the influence of many factors. The spatiotemporal expression of several transcription factors participates in pituitary development (Davis et al. 2010; de Moraes et al. 2012; Zhu et al. 2007) but a comprehensive understanding of the roles of these transcription factors and the mechanisms involved is as yet elusive.

Recently, we reported that a pituitary-specific transcription factor, PROP1 (Prophet of PIT1 [pituitary-specific transcription factor 1]), appears in *sex-determining region Y-box 2* (*Sox2*)-expressing stem/progenitor cells and fades away in the process of commitment to terminal differentiation in the rat embryonic pituitary (Yoshida et al. 2009), followed by localization in a part of SOX2-positive cell clusters (called a niche) in the parenchyma of the anterior lobe (Yoshida et al. 2011). PROP1 is considered to play important roles in the postnatal stem/progenitor cell niche (Chen et al. 2013; Higuchi et al. 2013; Yoshida et al. 2013, 2015). *Prop1* encodes a paired-like homeodomain transcription factor and is a heritable responsive gene for combined pituitary hormone deficiency in *Ames* dwarf mice (*Prop1*-deficient dwarf mice; Sornson et al. 1996) and human patients (Arroyo et al. 2002; Fluck et al. 1998; Wu et al. 1998), supporting the theory that it is probably a master gene of the pituitary. Studies of *Ames* dwarf mice have consistently shown that PROP1 is involved in morphogenesis, apoptosis and proliferation in the developing pituitary and in cell migration in the expanding anterior lobe from early embryogenesis through adulthood (Cushman et al. 2001). The study of molecules presenting in the downstream area of PROP1 action is an important means for clarifying the molecular mechanism of pituitary organogenesis. We focus our attention on a small protein, namely neuronatin (NNAT), because its expression level remarkably decreases in *Ames* dwarf mice (Sornson et al. 1996) and because it is well-known as a factor involved in early neurogenesis (Joseph et al. 1995).

Two splicing variants of NNAT encoding 81 amino acids (NNATα) and 58 amino acids (NNATβ) have been identified and their sequences are well evolutionarily conserved (Aikawa et al. 2003; Joseph et al. 1995). The amino acid sequences of both splicing variants show characteristic hydrophobic amino terminals and hydrophilic carboxy terminals and can be assumed to be membrane proteins in the endoplasmic reticulum (ER; Dou and Joseph 1996). In the neural stem cell line, NNAT has been

demonstrated to participate in neural differentiation by increasing intracellular Ca^{2+} through the inhibition of Ca^{2+} uptake in the ER by sarco/ER Ca^{2+} ATPase isoform 2 (SERCA2; Lin et al. 2010). Involvement in insulin secretion has also been reported by using β-cell lineage cells (Joe et al. 2008). On the other hand, *Nnat* transcripts in the pituitary have been detected to be as much as a 5th in abundance on a par with pituitary hormones (Nishida et al. 2005). *Nnat* null mice (MGI ID: 5007264) show no obvious defects indicating the presence of a molecule that plays a compensation action; this might pose difficulties for functional analysis. Nevertheless, investigations of NNAT in the pituitary so far have been too few to elucidate its function.

The present study aims to reveal *Nnat* expression and the localization of NNAT-positive cells in the rat embryonic and postnatal pituitaries. Abundant *Nnat* expression during embryonic development and its remarkable decrease after birth have been observed by real-time polymerase chain reaction (PCR). Immunohistochemistry has shown that NNAT appears in SOX2-positive stem/progenitor cells on embryonic day 11.5 (E11.5) and later exists in the majority of SOX2/PROP1-positive cells on E13.5, followed by localization in stem/progenitor cells, commitment cells and a small population of terminally differentiated cells during the progress of pituitary organogenesis. In the adult pituitary, NNAT exists in a limited number of SOX2-positive cells or in a few PIT1-positive commitment cells and non-hormone-producing cells and has been revealed, by localization, to occur in widespread subcellular organelles in addition to ER, as previously reported (Lin et al. 2010).

Materials and methods

Animals

Wistar-Imamichi strain male rats were housed individually in a temperature-controlled room under a 12-h light/12-h dark cycle. Determination of pregnancy was made by the observation of a vaginal plug on day 0.5 of gestation. Rats were killed by cervical dislocation under anesthesia. The present study was approved by the Institutional Animal Care and Use Committee, Meiji University, based on NIH Guidelines for the Care and Use of Laboratory Animals.

Quantitative real-time PCR

Total RNAs were prepared from whole pituitaries of E14.5 (*n*=10), E15.5 (*n*=17), E16.5 (*n*=14), E18.5 (*n*=11), E20.5 (*n*=10), E21.5 (*n*=8) and postnatal day 0 (P0, *n*=9) rats and from the anterior lobes and intermediate/posterior lobes of P15 (*n*=8), P30 (*n*=6) and P60 (*n*=3) rats by using ISOGEN (Nippon Gene, Tokyo, Japan). Reverse transcription and quantitative real-time PCR were performed as described previously (Yoshida et al. 2011). The specific primer sets

used were: rat $Nnat\alpha$ (forward primer; F) 5′-CATCATCGGCTGGTACATCTTC-3′ and (reverse primer; R) 5′-GCGAATCCTACCCAGTAAATGC-3′; rat $Nnat\beta$ (F) 5′-GTGCTGCTGCAGGTGTTCAGGTAC-3′ and (R) 5′-GGCATTGGCTCCCATGCTGG-3′; rat TATA-box-binding protein (Tbp; F) 5′-GATCAAACCCAGAATTGTTCTCC-3′ and (R) 5′- ATGTGGTCTTCCTGAATCCC-3′. Each sample was measured in duplicate in two independent experiments and data were calculated by the comparative C_T method (DDC$_T$ method) to estimate the mRNA level relative to that of Tbp as an internal standard. The DNA sequence of the PCR product of each sample was confirmed by nucleotide sequencing (data not shown).

Immunohistochemical analyses

Rat embryonic pituitaries and postnatal male rat pituitaries were removed, followed by fixation, dehydration and embedding as described previously (Yoshida et al. 2011). Frozen sections (10 μm thick) on glass slides (Matsunami, Osaka, Japan) were activated by an Immunosaver (Nisshin EM, Tokyo, Japan) for 60 min at 80 °C and washed three times in 20 mM HEPES, pH 7.5, containing 100 mM NaCl (HEPES buffer) for 10 min. This was followed by blocking with 0.4 % Triton-X (SIGMA-ALDRICH, Tokyo, Japan) and 10 % fetal bovine serum in HEPES buffer, pH 7.5, for 60 min at room temperature. Incubation with primary antibodies was performed for 16 h at 4 °C. Primary antibodies used were rabbit IgG against mouse neuronatin (1:250 dilution; ab27266, Abcam, Cambridge, UK), guinea pig IgG against rat PROP1 (2.5 ng/μl; Yoshida et al. 2011), mouse antiserum against human PRRX2 (1:1000 dilution; Abnova, Taipei City, Taiwan), mouse monoclonal IgG against rat PIT1 (1:50 dilution; Abcam), goat IgG against human SOX2 (1:500 dilution; Neuromics, Edina, Minn., USA), mouse monoclonal IgG against rat protein disulfide isomerase (PDI; 1:1000 dilution; Abcam) and mouse IgG against human Ki67 (1:100 dilution; BD Biosciences, San Jose, Calif., USA). Guinea pig antiserum against pituitary hormones: anti-human growth hormone (GH; 1:2000 dilution) and anti-human adrenocorticotropic hormone (ACTH; 1:5000 dilution) were kindly provided by Dr. S. Tanaka of Shizuoka University; anti-rat follicle-stimulating hormone (FSHβ; 1:10,000 dilution), rat luteinizing hormone (LHβ; 1:20,000 dilution), rat thyroid-stimulating hormone (TSHβ; 1:50,000 dilution) and rat prolactin (PRL; 1:10,000 dilution) were kindly provided by the National Institute of Diabetes and Digestive and Kidney Diseases (NIDDK) courtesy of Dr. A. F. Parlow. Anti-green fluorescent protein (GFP) antibody (chicken IgY against jellyfish GFP at 1:500 dilution; Aves Labs, Tigard, Ore., USA) was used to visualize enhanced yellow fluorescent protein (EYFP). After being washed with HEPES buffer three times, sections were incubated for 2 h at room temperature with Cy3, Cy5, or

fluorescein isothiocyanate (FITC)-conjugated donkey anti-rabbit, anti-guinea pig, anti-goat, anti-mouse IgG or anti-chicken IgY antibody (1:500 dilution) as secondary antibodies (Jackson ImmunoResearch, West Grove, Pa., USA). This was followed by enclosure in a Vectashield mounting medium containing 4′6-diamidino-2-phenylindole (DAPI; Vector, Burlingame, Calif., USA) and then observation by using fluorescence microscopy (BZ-9000, Keyence, Osaka, Japan) and fluorescence confocal microscopy (FV1000, OLYMPUS, Tokyo, Japan).

An absorption test of the anti-mouse NNAT polyclonal antibody was performed by using NNAT antibodies preabsorbed with its antigen, namely mouse NNAT peptide (amino acid number 35–81, ab30332, Abcam), at a 0.25 molar ratio against IgG.

Vector construction

Expression vectors for examining the localization of NNAT were constructed by fusing localization signal peptides (in reference to the Living Colors User Manual, PT2040-1, CLONTEC, Palo Alto, Calif., USA) to fluorescence protein (EYFP) of the pEYFP-C1 (CLONTEC). Expression vectors of NNAT and its truncates were constructed by making an insertion in the cloning site at the N- or C-terminus of EYFP of the pEYFP-C1.

Cell culture and transfection

The pituitary-tumor-derived gonadotrope cell line, LβT2 (kindly provided by Dr. P. L. Mellon, University of California-San Diego), was maintained as described previously (Sato et al. 2006). Cells were seeded at 2×10^4 in 0.1 ml Dulbecco's modified Eagle medium per well in a 16-well chamber glass slide (Thermo Scientific Nunc, Waltham, Mass., USA) for 24 h prior to transfection. Transfection was performed with 80 ng DNA (40 ng expression vector fused to EYFP and 40 ng empty pcDNA 3.1 Zeo$^+$ vector as a carrier)/ 0.3 μl FuGEN6 (Roche Diagnostic, Indianapolis, Ind., USA) per well as described previously (Susa et al. 2008). After incubation for 48 h at 37 °C, cells were fixed with 4 % paraformaldehyde in 20 mM HEPES for 30 min at room temperature, followed by immunocytochemistry with anti-GFP antibody.

Results

Expression profile of *Nnat* during pituitary development

The ontogeny of $Nnat\alpha$ and $Nnat\beta$ expression levels was analyzed by quantitative real-time PCR for total RNAs prepared from the pituitaries from E14.5 to P60 (Fig. 1). Expression of both isoforms was detected in the pituitary primordium on E14.5. At this time, $Nnat\alpha$ was highly expressed by about
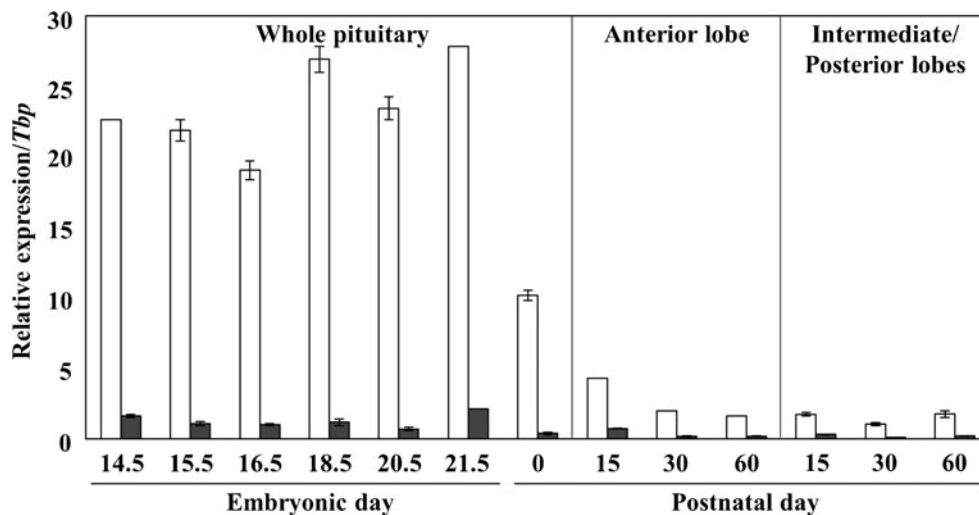
Fig. 1 Expression profile of *neuronatin* (*Nnat*) during rat pituitary development. Quantitative real-time polymerase chain reaction (PCR) was performed to estimate mRNA levels of two isoforms, *Nnatα* (*white bars*) and *Nnatβ* (*gray bars*), by using total RNAs prepared from whole pituitaries from embryonic day 14.5 (E14.5) to postnatal day 0 (P0) and

from anterior and intermediate/posterior lobes separately from P15 to P60. Data were calculated by the comparative C_T method to estimate the mRNA level relative to that of the TATA box binding protein gene (*Tbp*) used as an internal standard. Data are presented as the mean±SD of duplicate PCRs in two independent experiments

22.6-fold against *Tbp* (TATA-box binding protein as an internal marker), whereas *Nnatβ* was low at 1.6/*Tbp*. Between the *Nnat* isoforms, *Nnatα* expression in the pituitary was predominant throughout life and its high expression level was sustained until E21.5 (27.9/*Tbp*), followed by a marked decrease from P0 (10.2/*Tbp*) to P60 (1.6/*Tbp*). In the intermediate and posterior lobes, the *Nnatα* level was low at 1.7/*Tbp*

even on P15. These results indicate that NNAT actively plays a role in the embryonic pituitary.

Immunohistochemistry of NNAT in embryonic pituitaries

Specificity of the NNAT antibody was first examined for the cephalic part of the embryo on E16.5 by using antibodies pre-
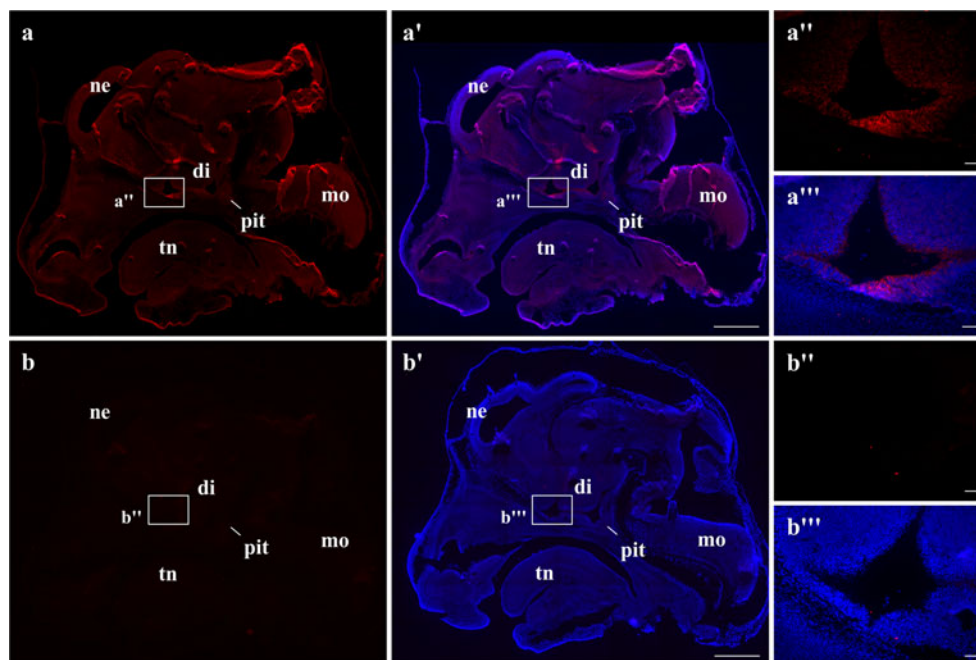

Fig. 2 Confirmation of specificity of anti-NNAT antibody. After fixation of the cephalic part of rat embryo on E16.5 in paraformaldehyde solution, sagittal sections were immunostained for NNAT. The signals for NNAT labeled with Cy3 (*red*) and the merged images with nuclei staining by 4′ 6-diamidino-2-phenylindole (DAPI, *blue*) are shown (**a-a′**; number of independent pituitaries assayed, *n*=1). Immunohistochemistry with

anti-NNAT antibody preabsorbed with the mouse NNAT peptide used as the antigen was also performed (**b-b′**). *Boxed areas* were enlarged (**a″** anti-NNAT antibody, **b″** absorbed antibody, **a‴, b‴** merged images with DAPI; *ne* neopallial cortex, *mo* medulla oblongata, *tn* tongue, *pit* pituitary, *di* diencephalon). *Bars* 1000 μm (**a′, b′**), 50 μm (**a″-a‴, b″-b‴**)

absorbed with antigen peptide. Whereas signals positive for NNAT were widely observed (Fig. 2a-a'''), pre-absorption removed the immunoreactive signals observed in the developing diencephalon and hypothalamus (Fig. 2b-b'''), confirming the specificity of the antibody used.

Subsequently, immunohistochemistry for NNAT was performed for the embryonic pituitaries (Fig. 3). In the invaginating oral ectoderm (a prospective pituitary primordium) at E11.5, NNAT signals were observed in a small number of cells in the cell layer facing the lumen (Fig. 3a-a', b-b'), unlike cells in the outer layer close to the diencephalon where PROP1-positive cells first appear (Yoshida et al. 2009). Two days later on E13.5, the intensity of NNAT signals increased in the majority of cells in the primordium of Rathke's pouch, except for the rostral tip and in the presumptive posterior lobe where PROP1-positive cells are absent (Yoshida et al. 2009; Fig.3c-c', d-d'). On E16.5, the number of NNAT-positive cells markedly increased in the expanding anterior lobe and almost 100 % of cells in the intermediate lobe were still positive for NNAT (Fig.3e-e', f-f'). By E20.5, although NNAT signals intensified but decreased in number in the intermediate lobe, a large number of NNAT-positive cells lined the marginal cell layer (MCL) and were scattered in the parenchyma of the anterior lobe (Fig.3g-g', i-i'). Previous investigators had shown

a high expression of NNAT in the ventral region in mouse pituitaries at E14.5-15.5 (Chu and Tsai 2005; Sornson et al. 1996) and an abundant expression in the ventral regions occurred after transient expression in the dorsal region in the rat pituitary. In addition, NNAT-positive cells were not detected in the pars tuberalis on E20.5 (Fig. 3h-h'). Notably, the intensity of NNAT signals in the presumptive posterior lobe and hypothalamus markedly increased on E13.5 and E16.5 compared with that on E11.5 but rapidly faded away by E20.5 (Fig. 3a, c, e, g).

Colocalization of NNAT with stem/progenitor cell markers, SOX2 and PROP1

We previously observed that PROP1 first appeared in the *Sox2*-expressing stem/progenitor cells in the primordium of Rathke's pouch on E11.5 and that all embryonic pituitary cells except for the rostral tip were positive for SOX2 and PROP1 on E13.5 (Yoshida et al. 2009, 2011). Hence, we examined the colocalization of NNAT with SOX2 and PROP1. NNAT was observed in SOX2/PROP1 double-positive cells on E12.5 (Fig.4a, b-b'''', closed arrowheads), after which NNAT-signals were detected in the majority of SOX2/PROP1 double-positive cells on E13.5 (Fig.4c, d-d'''',
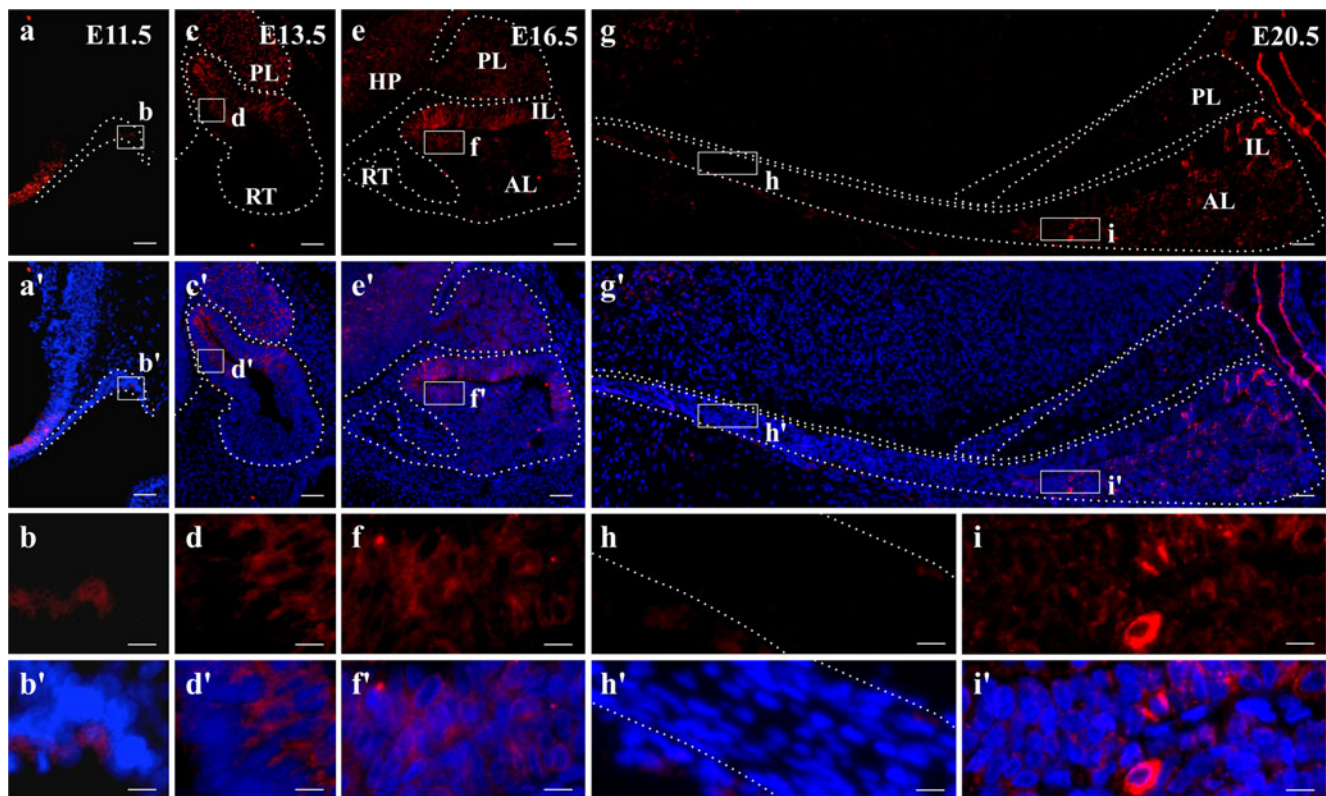

Fig. 3 Immunohistochemistry of NNAT during pituitary embryonic development. Immunohistochemistry of NNAT was performed with frozen sections in the sagittal plane prepared from pituitaries on E11.5 (**a** *n*=2), E13.5 (**c** *n*=2), E16.5 (**e** *n*=7) and E20.5 (**g** *n*=3) by visualization with Cy3 (*red*). Merged images with DAPI (*blue*) are shown (**a'**, **c'**, **e'**, **g'**). *Boxed areas* are enlarged in **b-b'**, **d-d'**, **f-f'**, **h-h'** and **i-i'**. *Dotted lines* indicate border of adenohypophysis and neurohypophysis (*AL* anterior lobe, *IL* intermediate lobe, *PL* posterior lobe, *HP* hypothalamus, *RT* rostral tip, *PT* pars tuberalis). *Bars* 50 μm (*1st, 2nd rows*), 10 μm (*3rd, 4th rows*)
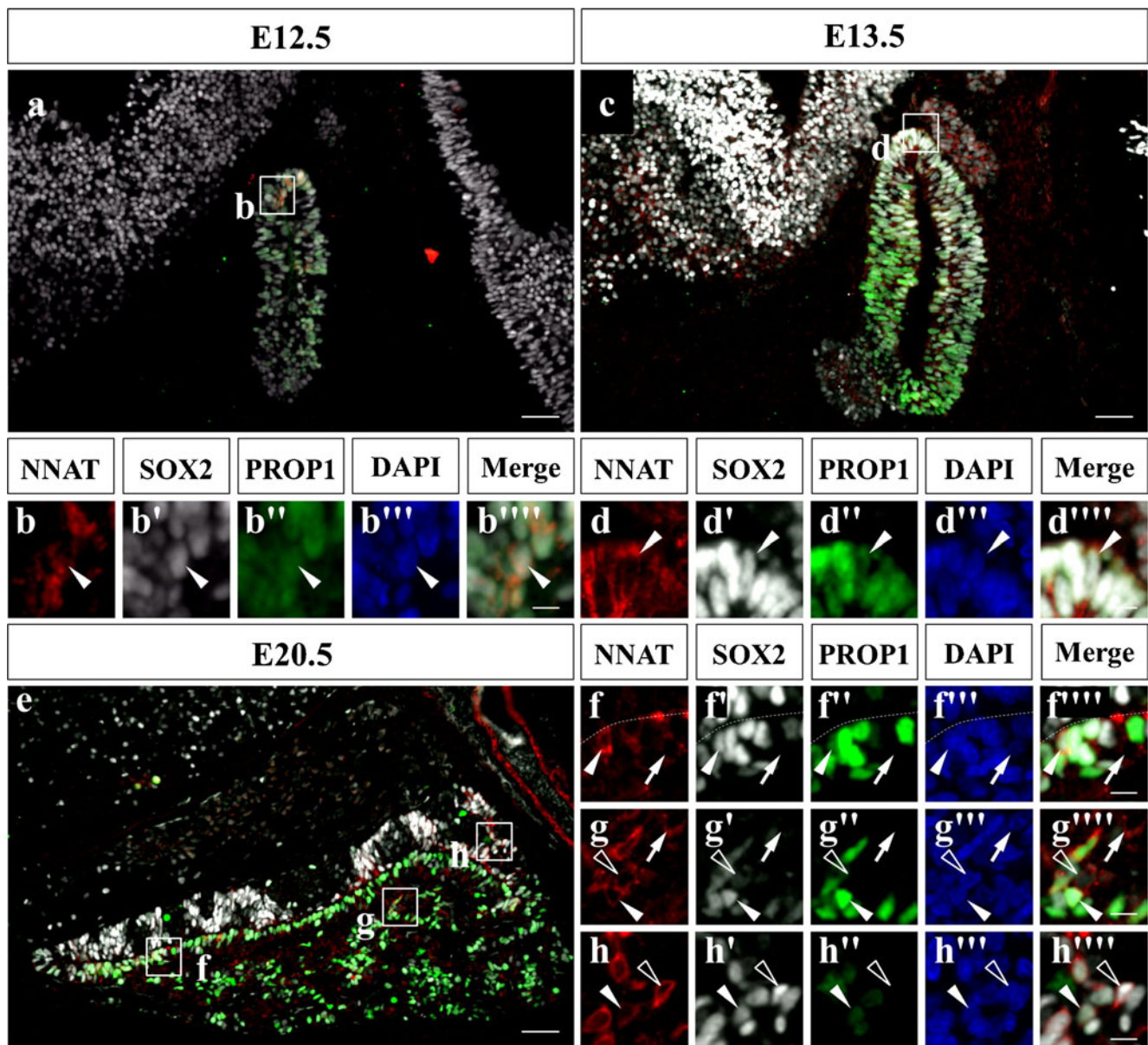
Fig. 4 Triple immunostaining of NNAT, SOX2 (sex-determining region Y-box 2) and PROP1 (Prophet of PIT1) in rat embryonic pituitaries. NNAT, SOX2 (a stem/progenitor cell marker) and PROP1 (a pituitary specific transcription factor) were visualized with Cy3 (*red*), fluorescein isothiocyanate (FITC, *white*) and Cy5 (*green*), respectively and with DAPI (*blue*) in closed arrowheads). On E20.5, localization of NNAT-positive sagittal sections of pituitaries on E12.5 (**a** *n*=1), E13.5 (**c** *n*=2) and E20.5 (**e** *n*=2). *Boxed areas* are enlarged (**b-b''''**, **d-d''''**, **f-f''''**, **g-g''''**, **h-h''''**). NNAT/SOX2/PROP1-triple (*closed arrowheads*), NNAT/SOX2 double-positive (*open arrowheads*) and NNAT single-positive (*arrows*) cells are indicated. *Bars* 50 μm (**a, c, e**), 10 μm (**b'''', d'''', f'''', g'''', h''''**)

cells showed significant alteration and NNAT/SOX2 double-positive cells particularly decreased in number in the intermediate lobe (Fig. 4e). In the anterior lobe (Fig.4f-f''', g-g'''') and intermediate lobe (Fig. 4h-h''''), not only NNAT/SOX2/PROP1 triple-positive cells (Fig.4f-f''', g-g'''', h-h'''', closed arrowheads) and NNAT/SOX2 double-positive cells (Fig.4g-g'''', h-h'''', open arrowheads) but also NNAT single-positive cells (Fig.4f-f''', g-g'''', arrows) were detected. These results together with those described above showed that NNAT was not a direct downstream target of PROP1.

Colocalization of PRRX1, a progenitor/commitment cell marker and PIT1, a commitment cell marker

We recently demonstrated that SOX2/PROP1 double-positive cells have a differentiation process that goes through a transitional state by expressing progenitor and commitment factors (Yoshida et al. 2009, 2011). To characterize the conversion of NNAT-positive cells during differentiation, immunohistochemistry was performed for paired-related homeobox 1 (PRRX1), a marker for pituitary progenitor/commitment cells (Higuchi et al. 2014; Susa et al. 2012) and mesenchymal

cells (de Jong and Meijlink 1993; Opstelten et al. 1991) and for PIT1, a marker for commitment cells that differentiate into GH-, PRL- and TSH-producing cells (Sornson et al. 1996). To examine triple staining, we used mouse anti-PRRX2 antibody that recognizes both PRRX1 and PRRX2 because of their sequence similarity (Susa et al. 2009). However, its positive signals were expected to show PRRX1-positive cells in the embryonic pituitary, since PRRX2-positive cells are absent in the embryonic pituitary, as described previously (Higuchi et al. 2014). NNAT signals were present in SOX2/PRRX1 double-positive cells in the MCL (Fig. 5a-a''', closed arrowheads) and parenchyma (Fig. 5b-b''', closed arrowheads), indicating that NNAT plays a role in the progenitor cells in a transition state. On the other hand, immunohistochemistry for PIT1 showed that PIT1-positive cells were absent from the MCL (Fig. 5c-c''') but were localized in the parenchyma of the anterior lobe (Fig. 5d-d'''). NNAT was present in PIT1-positive/SOX2-negative commitment cells beneath the MCL (Fig. 5c-c''', open arrowheads) and in the parenchyma of the anterior lobe (Fig. 5d-d''', open arrowheads), suggesting that NNAT performs its role as in the embryonic period in SOX2-positive cells to terminal differentiation.

Proliferative activity of NNAT-positive cells

Whether NNAT-positive cells have proliferative activity was examined by immunohistochemistry for NNAT and Ki67, a marker for cell proliferation (Fig. 6). By E16.5, most cells were Ki67/NNAT double-positive in the intermediate lobe and in the MCL of both lobes (Fig. 6a-a'', c). In the anterior lobe, proliferating NNAT-positive cells comprised about 86 % of proliferating cells, on E21.5 and the number of Ki67/NNAT double-positive cells (Fig. 6b-b'') markedly decreased by about 48 % (Fig. 6c). On the other hand, NNAT single-positive cells increased (Fig. 6c), indicating that NNAT does not directly correlate with cell proliferation.

Fig. 5 Triple immunostaining of NNAT, SOX2 and PRRX1 (paired-related homeobox 1) or PIT1 (pituitary-specific transcription factor 1) in rat embryonic pituitary. NNAT, SOX2 and PRRX1, a novel pituitary progenitor marker, or PIT1, a pituitary commitment cell marker, were visualized with Cy3 (NNAT; *red*), FITC (SOX2; *white*) and Cy5 (PRRX1 or PIT1; *green*) in sagittal sections of rat embryonic pituitary at E20.5 (*n*=3). Part of the marginal cell layer (*MCL*; **a-a'''**, **c-c'''**) and parenchyma (**b-b'''**, **d-d'''**) are shown. NNAT/SOX2/PRRX1 triple-positive (*closed arrowhead*), NNAT/PIT1 double-positive cells (*open arrowhead*), and MCL (*dotted line*) are indicated. *Bars* 10 μm
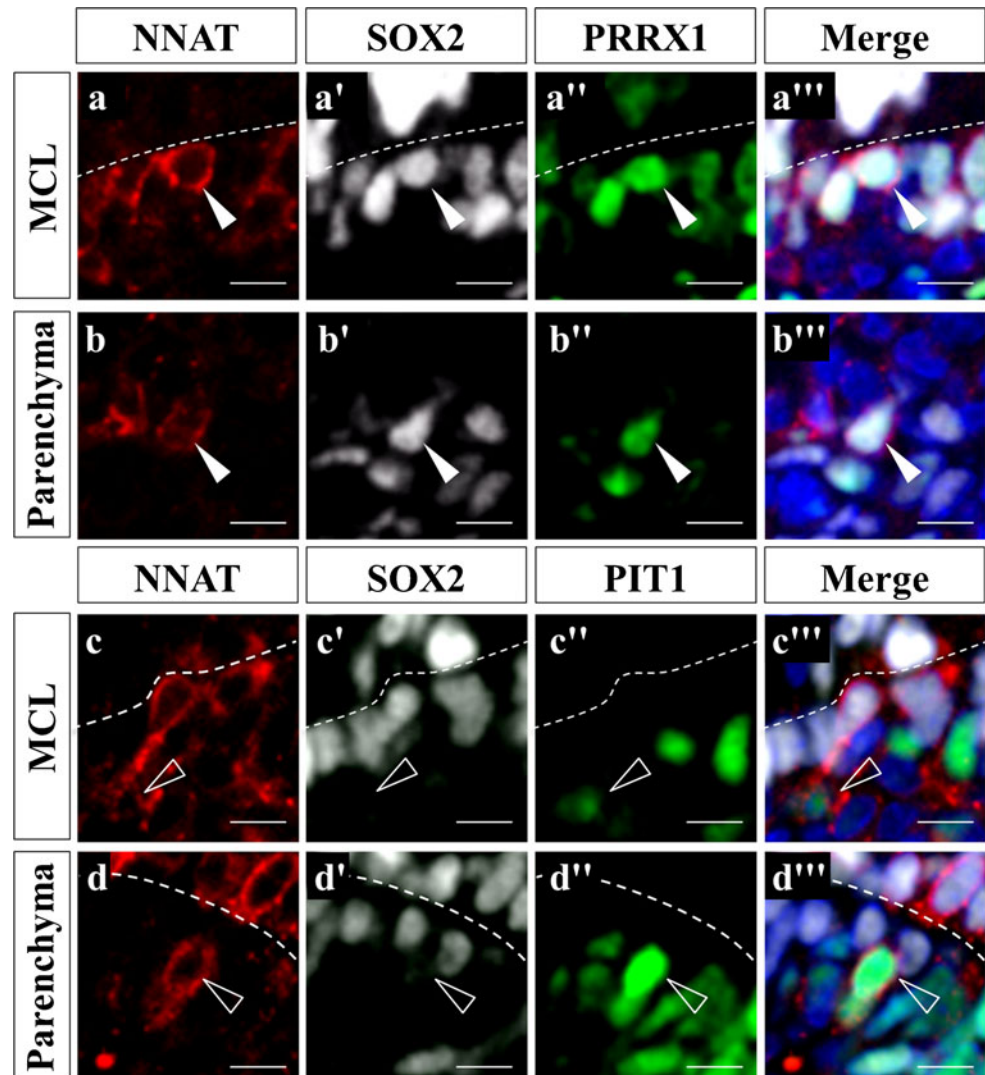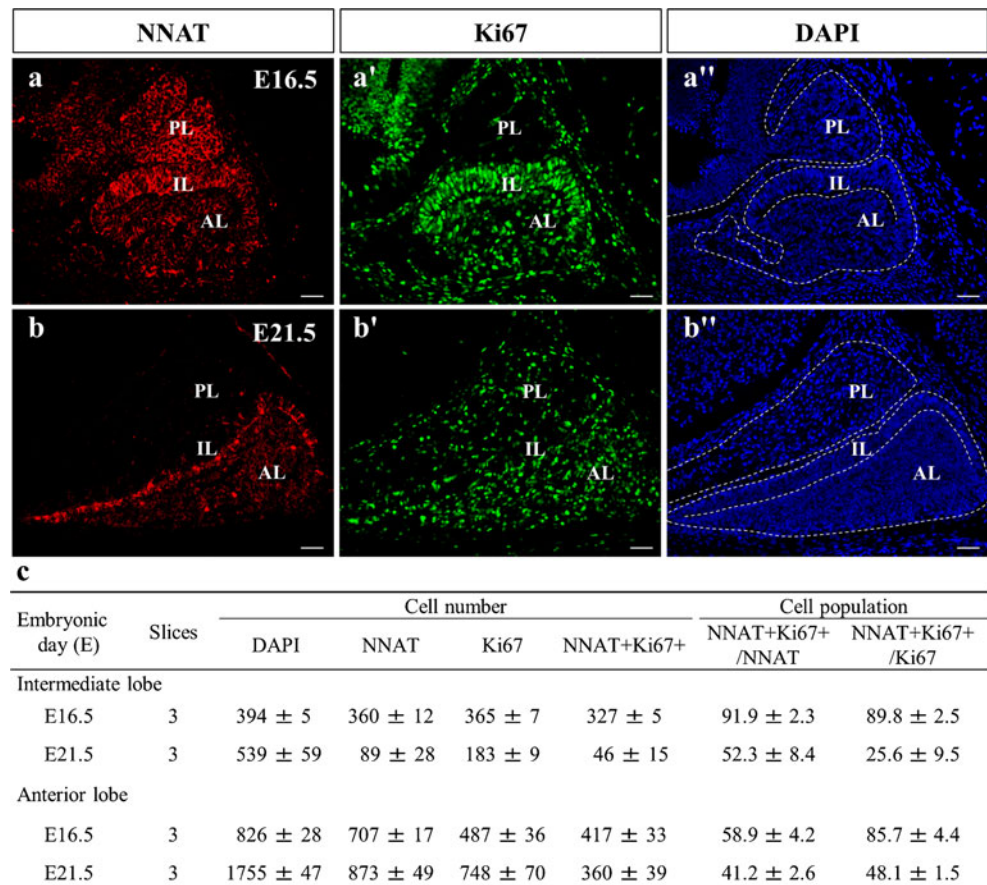
Fig. 6 Double immunostaining of NNAT and cell proliferation marker Ki67 in rat embryonic pituitaries. NNAT, Ki67 and nuclei were visualized with Cy3 (*red*), Cy5 (*green*) and DAPI (*blue*), respectively, in sagittal sections of rat pituitaries at E16.5 (**a-a''** *n*=2) and E21.5 (**b-b''** *n*=2; *AL* anterior lobe, *IL* intermediate lobe, *PL* posterior lobe). *Bars* 50 μm. **c** Numbers of cells positive for NNAT and for Ki67, double-positive for NNAT/Ki67 (*NNAT+Ki67+*) and positive for DAPI in the anterior and intermediate lobes on E16.5 and E21.5 were counted. Populations of NNAT/Ki67 double-positive cells among NNAT- or Ki67-positive cells are indicated

c

Embryonic day (E)	Slices	Cell number				Cell population	
		DAPI	NNAT	Ki67	NNAT+Ki67+	NNAT+Ki67+ /NNAT	NNAT+Ki67+ /Ki67
Intermediate lobe							
E16.5	3	394 ± 5	360 ± 12	365 ± 7	327 ± 5	91.9 ± 2.3	89.8 ± 2.5
E21.5	3	539 ± 59	89 ± 28	183 ± 9	46 ± 15	52.3 ± 8.4	25.6 ± 9.5
Anterior lobe							
E16.5	3	826 ± 28	707 ± 17	487 ± 36	417 ± 33	58.9 ± 4.2	85.7 ± 4.4
E21.5	3	1755 ± 47	873 ± 49	748 ± 70	360 ± 39	41.2 ± 2.6	48.1 ± 1.5

Colocalization of NNAT and hormones

During embryonic development from E15.5 to E21.5, all types of pituitary hormone-producing cells are terminally differentiated from stem/progenitor cells (Susa et al. 2012). Immunohistochemistry with a cocktail of antibodies against pituitary hormones, together with antibodies against NNAT and SOX2, was used to examine rat pituitary at E21.5 (Fig. 7a). Whereas NNAT signals were observed mostly in SOX2-positive cells, especially those lining the MCL and in SOX2/hormone double-negative cells in the parenchyma of the anterior lobe, NNAT/hormone double-positive cells were observed in the anterior lobe (Fig.7b-b''', c-c''', closed arrowheads) but not in the intermediate lobe, with only NNAT/SOX2 double-positive cells being located in this lobe (Fig. 7d-d''', open arrowheads). We further confirmed the colocalization of NNAT and hormones on the day when each hormone-producing cell first appeared (Fig. 7e, arrows). The data showed that NNAT functioned until the initiation of terminal differentiation.

Immunohistochemistry of NNAT in postnatal pituitary

Colocalization of NNAT with several of the factors analyzed in the embryonic pituitary, as described above, was examined in the postnatal pituitary. The number of NNAT-positive cells remarkably decreased in the postnatal anterior lobe and was extremely low in the intermediate lobe (data not shown), in contrast to their abundance in the embryonic intermediate lobe. Cell counting for double immunostaining images of NNAT and SOX2 in the anterior lobe was performed for areas of about 15,000-56,000 cells/1.5-5.4 mm^2 coronal section. The proportion of NNAT-positive cells was 0.06 % on P15, 0.03 % on P60 and 0.01 % on P71 (Fig. 8c). Representative immunostaining images are shown in Fig. 8. The proportion of NNAT/SOX2 double-positive cells among the NNAT-positive cells was 40 % (43/107 cells/9 sections) on P15 (Fig. 8a-a''', closed arrowheads) and 33 % (7/21 cells/5 sections) on P71 (Fig. 8b-b''', closed arrowheads). Furthermore, the NNAT single-positive cells remaining (14 cells) were present in the vicinity of SOX2-positive cells (Fig. 8b-b''', open arrowheads), indicating a direct correlation between NNAT- and SOX2-positive cells.

Double immunostaining with NNAT and PROP1 or PRRX1 did not show colocalization (data not shown) if this was any less than 10 %, because ≤10 NNAT-positive cells/section were observed in three sections of the postnatal anterior lobe. On the other hand, double immunostaining showed co-localization of NNAT and PIT1 proteins (Fig. 9a-a''', closed arrowheads) at a frequency of about 32 % (9 double-positive
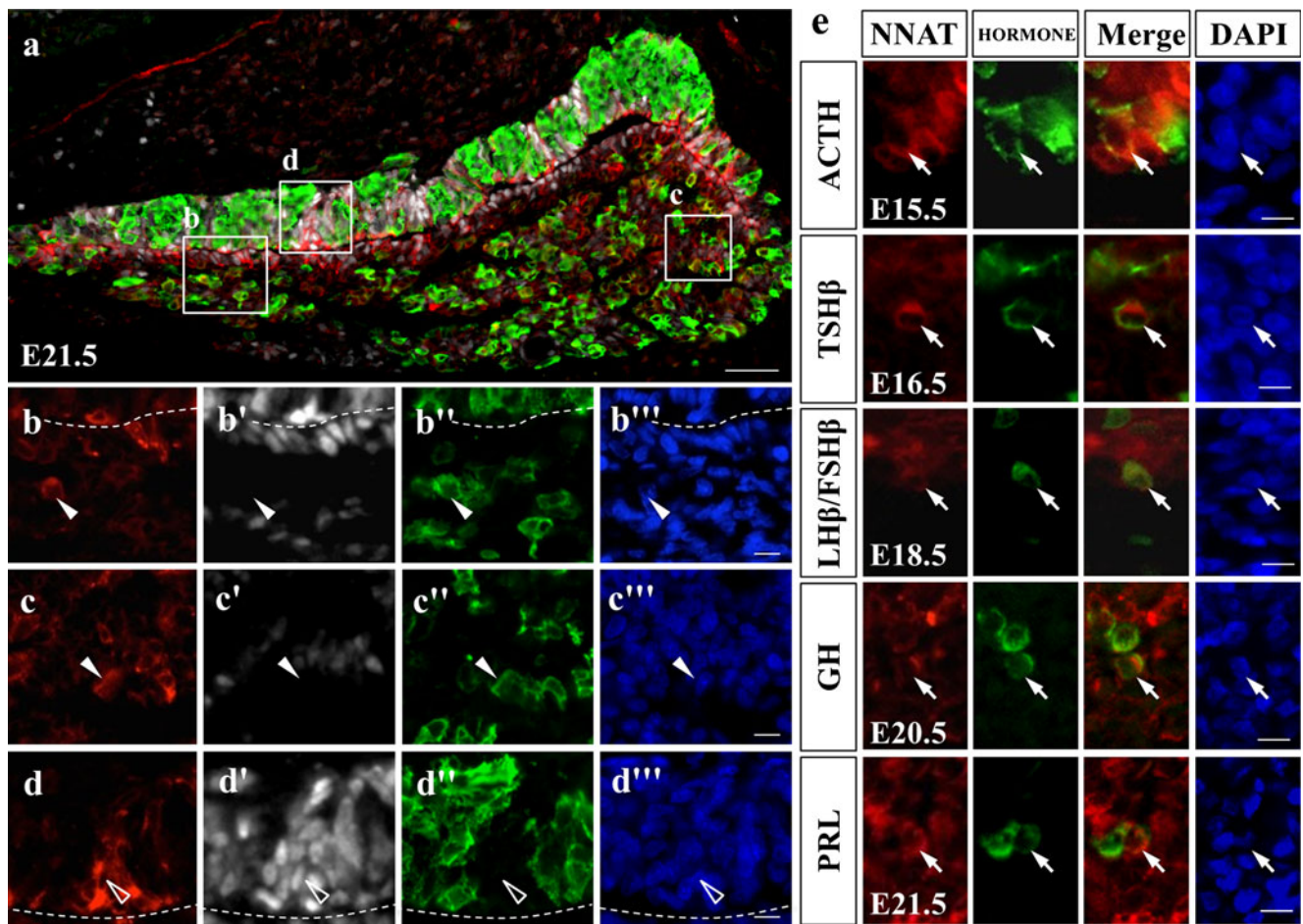
Fig. 7 Triple immunostaining of NNAT, SOX2 and hormones in rat embryonic pituitaries. Immunohistochemistry with a cocktail of antibodies against pituitary hormones (**a**) or antibody against individual hormones (**e**), together with antibodies against NNAT and/or SOX2, was performed in sagittal sections of rat embryonic pituitary on E15.5 (*n*=2), E16.5 (*n*=2), E18.5 (*n*=1), E20.5 (*n*=1) and E21.5 (*n*=3), followed by visualization with Cy3 (NNAT; *red*), Cy5 (SOX2; *white*) and FITC (each hormone; *green*). A merged image of NNAT, SOX2 and hormones is shown (**a**) with *boxed areas* being enlarged below (**b-b'''**, **c-c'''**, **d-d'''**).

Immunostaining for NNAT and each pituitary hormone is indicated in **e**. Embryonic days analyzed are indicated. NNAT/hormone double-positive/SOX2-negative (*closed arrowheads*), NNAT/SOX2 double-positive/hormone-negative (*open arrowheads*) and NNAT/hormone double-positive (*arrows*) cells are also indicated. *Bars* 50 μm (**a**), 10 μm (**b'''**, **c'''**, **d'''**, **e**) (*GH* growth hormone, *PRL* prolactin, *TSHβ* thyroid-stimulating hormone, *ACTH* adrenocorticotropic hormone, *LHβ/FSHβ* luteinizing hormone/follicle-stimulating hormone)
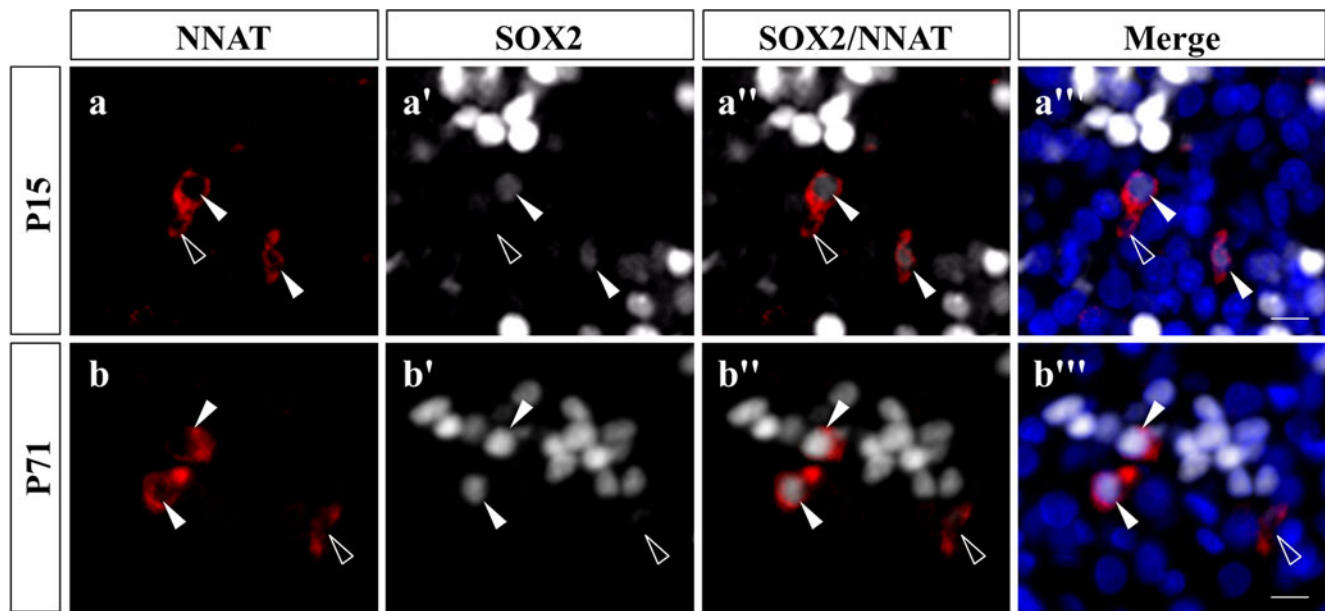
cells/28 NNAT-positive cells/3 coronal sections) on P62. In addition, immunohistochemistry of NNAT and each pituitary hormone was performed. Co-localization of NNAT and each pituitary hormone (Fig.9b-b''', c-c''', d-d''', e-e''', f-f''', closed ar-rowheads), similar to that in the embryonic pituitaries (Fig. 7), was observed among small numbers of NNAT-positive cells (0.01-0.02 %). As indicated in Fig. 9g, the proportion of NNAT/hormone double-positive cells was about 6-14 % of the NNAT-positive cells, with roughly a two-fold difference.

Intracellular localization of NNAT

Localization of NNAT in the ER has been postulated by using the pancreatic cell line (Joe et al. 2008). We reconfirmed the intracellular localization of NNAT in the pituitary (E18.5) by immunohistochemistry with an antibody against PDI, an ER

marker (Fig. 10a). Three-dimensional image analysis confirmed the colocalization of NNAT and PDI in the ER (Fig. 10c-c'', closed arrowheads). In addition, we observed both NNAT and PDI single-positive granules in the same image (Fig. 10b-b'', c-c'', open arrowheads and arrows, respectively), indicating the possibility that NNAT localizes in intracellular granules other than those associated with the ER.

To investigate further the subcellular localization in the ER, mitochondria, peroxisome, lysosome and Golgi, expression vectors that fused each localization signal peptide into EYFP were constructed and transfected into LβT2 cells in which NNAT existed. Colocalization was analyzed by immunocytochemistry with antibodies against NNAT and against GFP, which cross-reacts with EYFP (Fig. 11). In the LβT2 cells transfected with an empty vector, EYFP signals were located over the entire region of the cells including their nuclei

Fig. 8 Localization of NNAT in rat postnatal pituitary. Immunostaining for NNAT (*red* in **a**, **b**) and SOX2 (*white* in **a'**, **b'**) was performed with rat pituitary on P15 (*n*=2) and P71 (*n*=2). Merged images (**a"**, **b"**) and those with DAPI (*blue* in **a'''**, **b'''**) are shown. NNAT/SOX2 double-positive (*closed arrowheads*) and NNAT single-positive (*open arrowheads*) cells are indicated. *Bars* 10 μm. **c** Numbers of cells positive for NNAT and SOX2, double-positive for NNAT/SOX2 (*NNAT+SOX2+*) and positive for DAPI in slices of the anterior lobes on P15, P60 and P71 were counted. Populations of NNAT-positive cells among DAPI-positive cells and of NNAT/SOX2 double-positive cells among NNAT-positive cells are indicated. Total numbers of positive cell are indicated, as are the total number of measured pituitary slices

(Fig.11a-a''', b). NNAT-immunopositive signals colocalized with GFP signals localized in the ER (Fig.11c-c''', d), mito-chondria (Fig. 11e-e''', f), peroxisome (Fig.11g-g''', h), and a part of the lysosome (Fig.11i-i''', j), except for the Golgi (Fig.11k-k''', l). The data revealed that NNAT was mainly present in the mitochondria and ER.

The amino acid sequence of NNAT shows a characteristic structure: amino- and carboxy-termini are hydrophobic and hydrophilic, respectively (Fig. 12a). *Nnat* vectors fused with EYFP at either terminus were transfected into LβT2 cells to search for the region important for localization in the intracel-lular granules. Immunoreacted signals for endogenous NNAT and EYFP fused with a localization signal peptide for the Golgi are shown in Fig. 11k-k''', l. *Nnat* vectors of α- and β-isoforms fused with EYFP at the carboxy-terminus exhibited granular localizations (Fig. 12c-c'), similar to those of endog-enous NNAT (Fig. 12b-b''', *red*). On the other hand, those fused to EYFP at the amino-terminus showed an unusual ac-cumulation at the Golgi (Fig. 12d-d', closed arrowheads), as

shown in Fig. 12b-b''' (*green*). Whereas deletion of the hydro-phobic region (residue 1–38) exhibited localization over the entire area of the cell including the nucleus (Fig. 12c''', d'''), deletion of the hydrophilic region (reside 39–81) showed a localization similar to endogenous NNAT (Fig. 12c", d"), in-dicating that the hydrophobic region is predominant for intra-cellular localization.

Fig. 9 Localization of NNAT in rat postnatal pituitary. Immunostaining ▶ for NNAT (*red* in **a, b, c, d, e, f**) and PIT1 or hormones (*white or green*, respectively, in **a', b', c', d', e', f'**) was performed with rat pituitary on P62 (*n*=4). Merged images (**a", b", c", d", e", f"**) and those with DAPI (*blue* in **a''', b''', c''', d''', e''', f'''**) are shown. *Closed arrowheads* indicate NNAT/PIT1 or hormone double-positive cells. *Open arrowheads* NNAT-positive only cell. *Bars* 10 μm. **g** Numbers of cells positive for NNAT, PIT1, pituitary hormones, double-positive cells for NNAT and PIT1 or pituitary hormones (*NNAT+ each factor+*), positive for DAPI were counted in slices. Populations of NNAT-positive cells among DAPI-positive cells and of NNAT/each factor double-positive cells among NNAT-positive cells are indicated
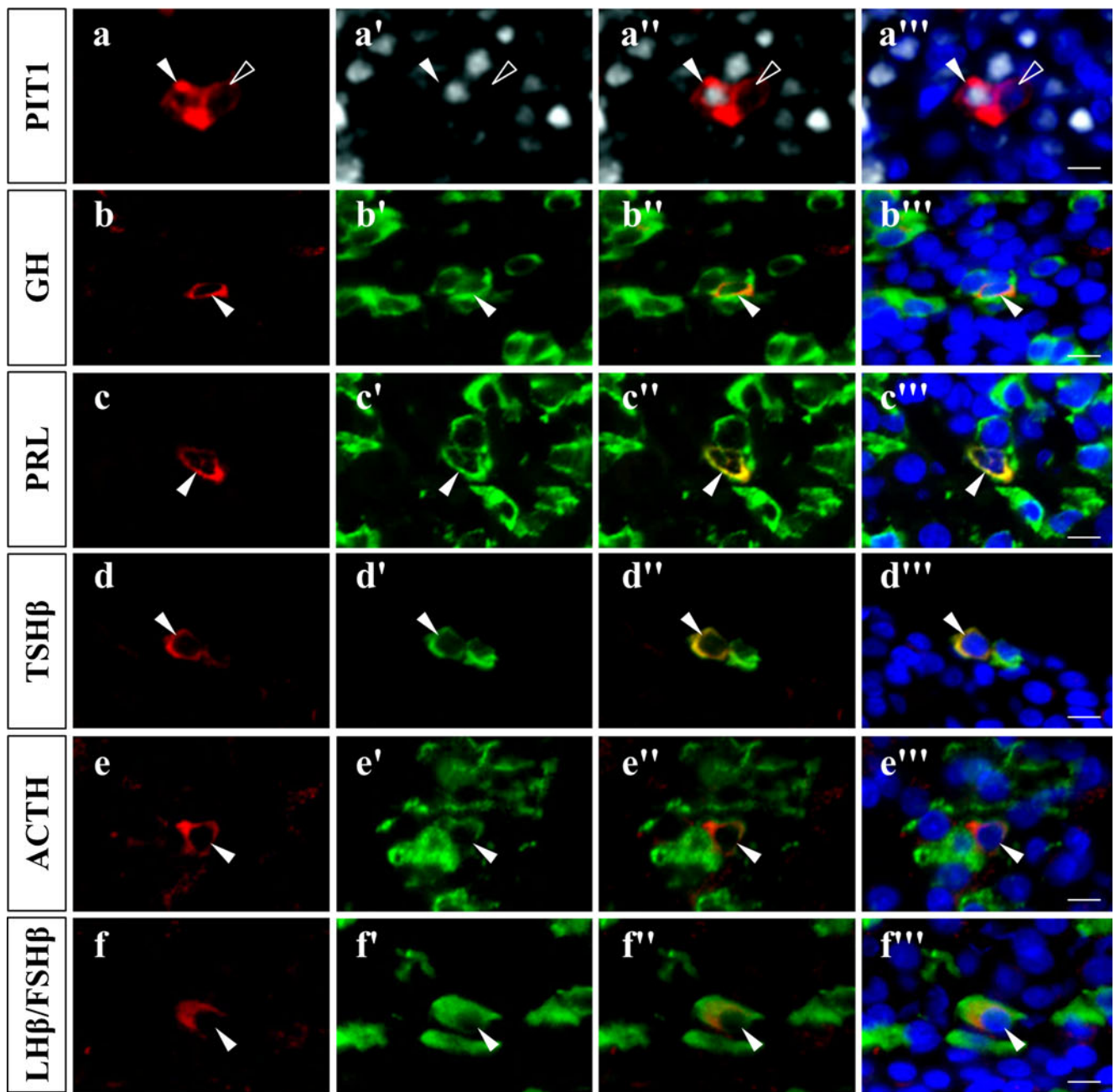
Factor	Slices	Cell number			Cell population (%)	
		DAPI	NNAT	NNAT+ each factor+	NNAT/DAPI	NNAT+ each factor+ /NNAT
PIT1	3	125617	28	9	0.02	32.1
GH	27	1168652	127	8	0.01	6.3
PRL	11	438420	54	4	0.01	7.4
TSH	8	327962	29	4	0.01	13.8
ACTH	4	212099	16	1	0.01	6.3
LH/FSH	2	108568	9	1	0.01	11.1

Fig. 10 Intracellular localization of NNAT in rat pituitary. Double immunostaining of NNAT and protein disulfide isomerase (PDI), an endoplasmic reticulum (ER) marker, in the sagittal section of rat embryonic pituitary on E18.5 was performed. NNAT and PDI were visualized with Cy3 (*red*) and Cy5 (*green*), respectively and merged images with DAPI (*blue*) are shown. Colocalization was confirmed with orthogonal projection by Z-stack imaging with 0.124-μm thickness (**b-b''**, **c-c''**). NNAT/PDI double-positve (*closed arrowhead*), NNAT single-positive (*open arrowhead*) and PDI single-positive (*arrow*) signals are indicated. *Bar* 5 μm
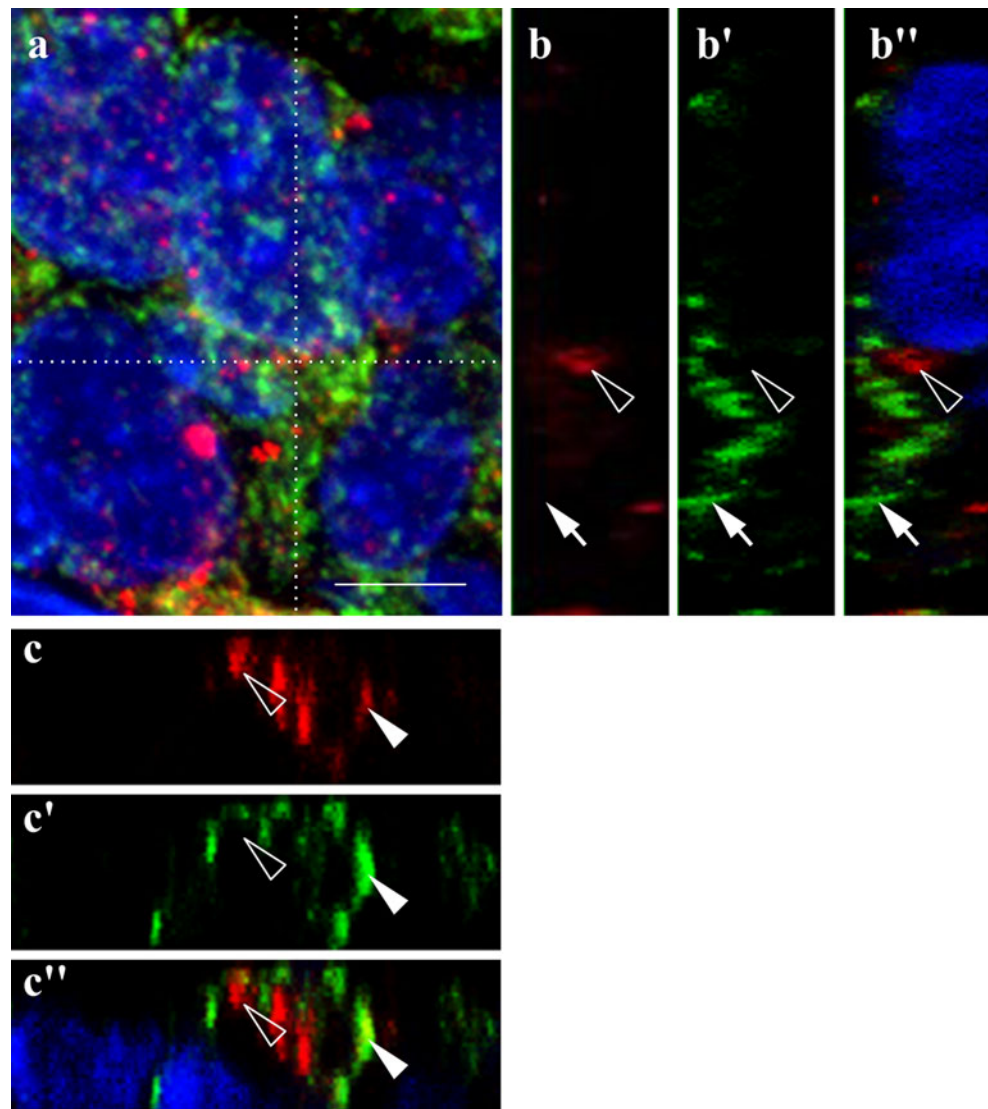

Discussion

NNAT has received attention because of its remarkable expression in the neonatal brain (Joseph et al. 1994; Usui et al. 1996; Wijnholds et al. 1995) and the pituitary (Nishida et al. 2005). However, the role of NNAT in the pituitary gland is poorly understood. In the present study, we demonstrated that NNAT appears in the SOX2-positive embryonic stem/progenitor cells on E11.5 and disappears at the initiation of terminal differentiation into hormone-producing cells in the embryonic pituitary, suggesting that the role of NNAT is closely associated with the differentiation process from pituitary stem/progenitor cell. After birth, the number of NNAT-positive cells remarkably decreases, suggesting that NNAT is not involved in the postnatal pituitary growth wave. However, NNAT presumably participates in the regeneration mechanism of the adult pituitary, because NNAT/SOX2 double-positive cells reside in the adult pituitary. Furthermore, the

present study is the first to suggest that NNAT is widely distributed in cell organelles, such as the mitochondria, peroxisome, a part of the lysosome and the ER and that the hydrophobic amino-terminus region of NNAT is important for its subcellular localization.

We were encouraged to undertake the present study because of results obtained by using the *Ames* dwarf mouse showing that a defect in *Prop1* causes a decrease in *Nnat* expression in the pituitary (Sornson et al. 1996). We confirmed that *Nnat* starts to appear in the SOX2-positive stem/progenitor cells and does not necessarily keep in phase with *Prop1* expression, revealing the loose relationship between the two proteins in stem/progenitor cells. Therefore, the decreased expression of *Nnat* in the *Ames* mouse suggests that PROP1 has an indirect role. Notably, Chu and Tsai (2005) demonstrated that *Nnat* expression in the pancreas is regulated by NeuroD1, a transcription factor expressed in both the pancreas and

Fig. 11 Intracellular localization of NNAT in pituitary gonadotrope-lineage cell line LβT2. Localization vectors that encoded five types of localization signal sequence fused to fluorescence protein (*YFP* enhanced yellow fluorescent protein; *green*) were transfected into LβT2 cells. Vectors encoding empty YFP (control; **a-a'''**, **b**) and YFP fused with signal sequence for ER (**c-c'''**, **d**), mitochondria (**e-e'''**, **f**), peroxisome (**g-g'''**, **h**), lysosome (**i-i'''**, **j**) and Golgi (**k-k'''**, **l**) were transfected into the cells. NNAT and EYFP were visualized with Cy3 (NNAT; *red*) and FITC (EYFP; *green*). Merged images with or without DAPI (*blue*) are shown. Colocalization was confirmed with orthogonal projection by confocal Z-stack imaging with 0.124-μm thickness (**b**, **d**, **f**, **h**, **l**) at *dotted* positions (**a'''**, **c'''**, **e'''**, **g'''**, **k'''**). NNAT-signals localized with (*closed arrowhead*) or without (*open arrowhead*) intracellular localization signals are indicated. *Bars* 5 μm
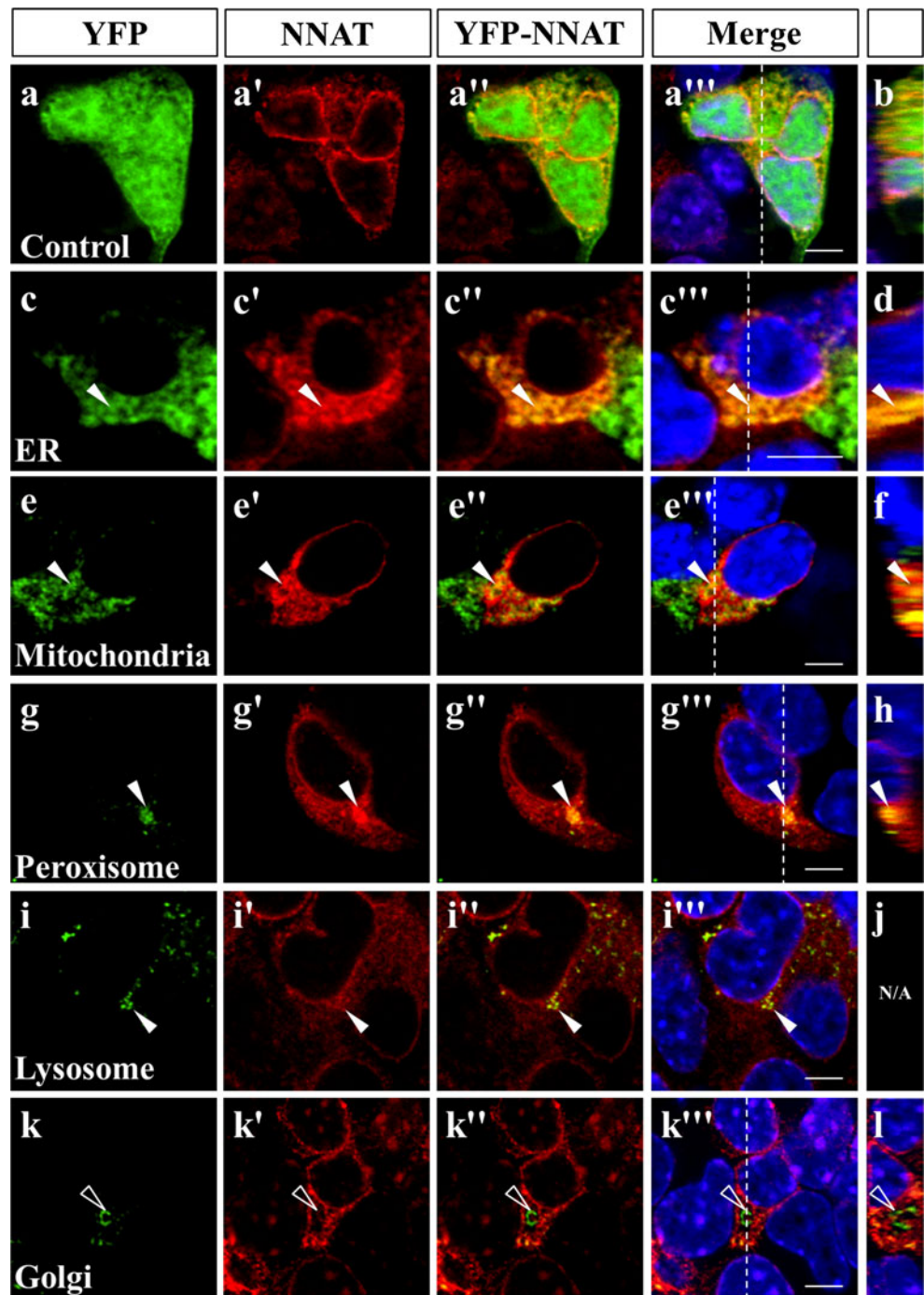
pituitary. However, the regulation of *Nnat* by NeuroD1 in the pituitary has thus far not been reported.

The ontogeny of *Nnat* expression in the pituitary gland by real-time PCR displays a higher expression level in the embryonic pituitary than in the adult pituitary. The result seems to be inconsistent with a previous report (Nishida et al. 2005) that *Nnat* is ranked as the fifth level (about 6 % of GH expression) in the expressed genes of the mouse anterior pituitary at 12–15 weeks. This discrepancy can be explained on the basis of the difference in species used (rat vs. mouse) and/or in the

quantitative methods employed (quantitative real-time PCR vs. serial analysis of gene expression tags, which causes a possible bias in amplification). We performed microarray analysis of the RNAs of rat anterior pituitary at P60 and found that the expression level of *Nnat* is about 8 % of GH expression (unpublished data). Accordingly, the result of the mouse pituitary is plausible. NNAT in the embryonic posterior lobe shows a transient appearance with prompt fading by E21.5. In the embryonic intermediate lobe, the number of NNAT signals reaches a maximum at around E16.5 and thereafter weak

Fig. 12 Determination of region in NNAT involved in intracellular localization. **a** Hydropathy profile (*top*), amino acid sequence (*middle*; deletion region in NNATβ is indicated in *red*) and diagram (*bottom*) with hydrophobic (*yellow* 1–38 residues) and hydrophilic regions (*blue* 39–81 residues). **b** Immunostaining of endogenous NNAT (*red* with Cy3) in LβT2 cells transfected by the localization vector for Golgi (*green*). Orthogonal projections by confocal Z-stack images with 0.124-μm thickness (**b'-b'''**) are shown. Transfection of expression vectors fused with EYFP at the carboxyl (**c-c'''**) and amino (**d-d'''**) termini of NNAT (NNATα: **c, d**; NNATβ: **c', d'**) or its deleted constructs was performed in LβT2 cells. Immunostaining images of EYFP visualized with Cy3 (*red*) merged with DAPI (*blue*) are shown. LβT2 cells transfected with EYFP-expression vectors fused with hydrophobic (**c'', d''**) and hydrophilic (**c''', d'''**) regions are also shown. *Closed arrowheads* indicate signals in Golgi. *Bars* 5 μm
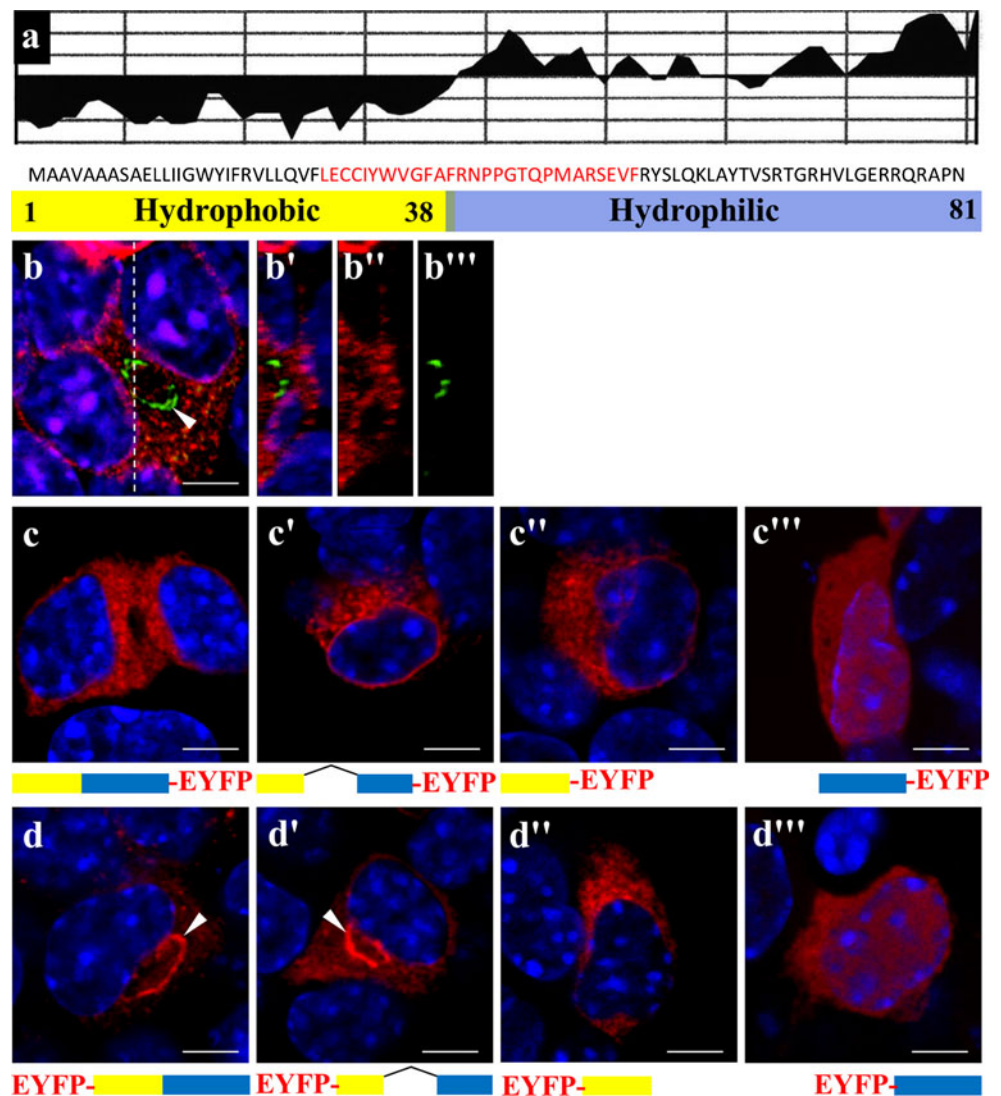
signals are still localized in non-endocrine cells. In contrast, NNAT-positive cells are scattered in the embryonic anterior lobe on E21.5, followed by a prompt decrease in number after birth. This contrasting temporospatial profile of NNAT in each lobe might correspond to the different mechanisms taking place in the organogenesis of each lobe. Collectively, the present study demonstrated that NNAT is present in the transition process from stem/progenitor cell to commitment cell and terminates its presence at the initiation of terminal differentiation during embryonic pituitary development. To clarify the potential role of NNAT during the transition from stem/progenitor cell to each hormone-producing cell, investigations involving the physiologically changed pituitary, such as during the estrous cycle, pregnancy, lactation/weaning, stress and/or estrogen-induced prolactinoma, in the future may provide novel clues. In support of our hypothesis, several investigators have reported that NNAT participates in tissue differentiation, such as potentiation for adipogenesis (Suh et al. 2005), promotion of neural lineage induction from embryonic

stem cells (Lin et al. 2010) and differentiation of keratinocytes (Dugu et al. 2014).

The molecular mechanism behind NNAT function is an important issue. Regulation of the intracellular Ca^{2+} concentration by NNAT exhibits the potential regulation of neuronal excitability, receptor trafficking and Ca^{2+}-dependent signaling involved in synaptic plasticity (Oyang et al. 2011). Co-immunoprecipitation assay with NNAT antibody has demonstrated that NNAT interacts with SERCA2 (Lin et al. 2010) and since SERCA2 transfers Ca^{2+} from the cytosol into the Ca^{2+}-rich lumen of the ER by acting as an adenosine-triphosphate-dependent Ca^{2+} pump, the interaction with NNAT antagonizes SERCA2 function and prevents Ca^{2+} influx to the lumen, resulting in a high Ca^{2+} concentration in the cytosol. Lin et al. (2010) demonstrated that an increased concentration of cytosolic Ca^{2+} stimulated by NNAT initiates neural induction in embryonic stem cells and that the *Nnat* expression level shows a bell-shaped curve together with progression

of neural induction. Indeed, an obstruction of differentiation by decreasing the intracellular Ca^{2+} concentration has been demonstrated with an overexpression of SERCA2 (Wang et al. 2014). Localization of immunopositive NNAT signals in the anterior and intermediate lobes and in the posterior lobe in the developing embryonic pituitary gland exhibits transition profiles similar to those in neural differentiation. Although further functional evidence is essential, NNAT in the pituitary stem/progenitor cells may have a comparable role with regard to intracellular Ca^{2+} in order for developmental organization and differentiation to continue.

NNAT has thus far been supposed to reside in ER (Joe et al. 2008; Suh et al. 2005). The presence of NNAT in another unidentified cellular structure has also been postulated (Chu and Tsai 2005). The present study has shown that NNAT localizes in additional subcellular organelles, such as the mitochondria, peroxisome and lysosome but not in the Golgi. This will be clarified by other approaches, such as immune-electron microscopy with high-quality antibody or fluorescence resonance energy transfer (FRET). The discrepancy with the previous observation might be corrected by improving the resolution of stereoscopic observation when using fluorescence microscopy and/or fluorescence confocal microscopy. The present study suggests that many intracellular granules contain molecules that interact with NNAT and that these interaction profiles lead to functions of NNAT other than the inhibition of Ca^{2+} influx. Furthermore, we confirmed that the hydrophobic N-terminal region of NNAT is predominant for intracellular localization.

In addition to the known role of NNAT in embryonic tissue development, the enhancement of insulin secretion by NNAT has also been demonstrated in the MIN6N8 insulinoma cell line (Joe et al. 2008). Indeed, although the increased *Nnat* expression in the embryonic tissues mostly decreases during the progression of development, we confirmed that some adult tissues still display significant expression (unpublished observations). Only specific cells and/or adult tissues might require the modulation of the intracellular Ca^{2+} concentration by NNAT or unidentified function(s) of NNAT for tissue regeneration and secretion. Nevertheless, the clarification of the molecular mechanisms involved in NNAT function(s), especially in the pituitary stem/progenitor cells, remains a significant issue in our understanding of pituitary organogenesis.

References

Aikawa S, Kato T, Elsaeesser F, Kato Y (2003) Molecular cloning of porcine neuronatin and analysis of its expression during pituitary ontogeny. Exp Clin Endocrinol Diabetes 111:1–5

Arroyo A, Pernasetti F, Vasilyev VV, Amato P, Yen SS, Mellon PL (2002) A unique case of combined pituitary hormone deficiency caused by a PROP1 gene mutation (R120C) associated with normal height and absent puberty. Clin Endocrinol (Oxf) 57:283–291

Chen M, Kato T, Higuchi M, Yoshida S, Yako H, Kanno N, Kato Y (2013) Coxsackievirus and adenovirus receptor-positive cells compose the putative stem/progenitor cell niches in the marginal cell layer and parenchyma of the rat anterior pituitary. Cell Tissue Res 354:823–836

Chu K, Tsai M-J (2005) Neuronatin, a downstream target of BETA2/NeuroD1 in the pancreas, is involved in glucose-mediated insulin secretion. Diabetes 54:1064–1073

Cushman LJ, Watkins-Chow DE, Brinkmeier ML, Raetzman LT, Radak AL, Lloyd RV, Camper SA (2001) Persistent Prop1 expression delays gonadotrope differentiation and enhances pituitary tumor susceptibility. Hum Mol Genet 10:1141–1153

Davis SW, Castinetti F, Carvalho LR, Ellsworth BS, Potok MA, Lyons RH, Brinkmeier ML, Raetzman LT, Carninci P, Mortensen AH, Hayashizaki Y, Arnhold IJ, Mendonca BB, Brue T, Camper SA (2010) Molecular mechanisms of pituitary organogenesis: in search of novel regulatory genes. Mol Cell Endocrinol 323:4–19

de Jong R, Meijlink F (1993) The homeobox gene S8: mesoderm-specific expression in presomite embryos and in cells cultured in vitro and modulation in differentiating pluripotent cells. Dev Biol 157:133–146

de Moraes DC, Vaisman M, Conceicao FL, Ortiga-Carvalho TM (2012) Pituitary development: a complex, temporal regulated process dependent on specific transcription factors. J Endocrinol 215:239–345

Dou D, Joseph R (1996) Cloning of human neuronatin gene and its localization to chromosome-20q 11.2-12: the deduced protein is a novel "proteolipid". Brain Res 723:8-22

Dugu L, Nakahara T, Wu Z, Uchi H, Liu M, Hirano K, Yokomizo T, Furue M (2014) Neuronatin is related to keratinocyte differentiation by up-regulating involucrin. J Dermatol Sci 73:225–231

Fluck C, Deladoey J, Rutishauser K, Eble A, Marti U, Wu W, Mullis PE (1998) Phenotypic variability in familial combined pituitary hormone deficiency caused by a PROP1 gene mutation resulting in the substitution of Arg→Cys at codon 120 (R120C). J Clin Endocrinol Metab 83:3727–3734

Higuchi M, Kato T, Chen M, Yako H, Yoshida S, Kanno N, Kato Y (2013) Temporospatial gene expression of Prx1 and Prx2 is involved in morphogenesis of cranial placode-derived tissues through epithelio-mesenchymal interaction during rat embryogenesis. Cell Tissue Res 353:27–40

Higuchi M, Yoshida S, Ueharu H, Chen M, Kato T, Kato Y (2014) PRRX1 and PRRX2 distinctively participate in pituitary organogenesis and cell supply system. Cell Tissue Res 357:323–335

Joe MK, Lee HJ, Suh YH, Han KL, Lim JH, Song J, Seong JK, Jung MH (2008) Crucial roles of neuronatin in insulin secretion and high glucose-induced apoptosis in pancreatic beta-cells. Cell Signal 20:907–915

Joseph R, Dou D, Tsang W (1994) Molecular cloning of a novel mRNA (neuronatin) that is highly expressed in neonatal mammalian brain. Biochem Biophys Res Commun 201:1227–1234

Joseph R, Dou D, Tsang W (1995) Neuronatin mRNA: alternatively spliced forms of a novel brain-specific mammalian developmental gene. Biomed Res 690:92–98

Lin HH, Bell E, Uwanogho D, Perfect LW, Noristani H, Bates TJ, Snetkov V, Price J, Sun YM (2010) Neuronatin promotes neural lineage in ESCs via Ca(2+) signaling. Stem Cells 28:1950–1960

Nishida Y, Yoshioka M, St-Amand J (2005) The top 10 most abundant transcripts are sufficient to characterize the organs functional specificity: evidences from the cortex, hypothalamus and pituitary gland. Gene 344:133–141

Opstelten DJ, Vogels R, Robert B, Kalkhoven E, Zwartkruis F, de Laaf L, Destree OH, Deschamps J, Lawson KA, Meijlink F (1991) The mouse homeobox gene, S8, is expressed during embryogenesis predominantly in mesenchyme. Mech Dev 34:29–41

Oyang EL, Davidson BC, Lee W, Poon MM (2011) Functional characterization of the dendritically localized mRNA neuronatin in hippocampal neurons. PLoS One 6:e24879

Sato T, Kitahara K, Susa T, Kato T, Kato Y (2006) Pituitary transcription factor Prop-1 stimulates porcine pituitary glycoprotein hormone α gene expression. J Mol Endocrinol 37:341–352

Sornson MW, Wu W, Dasen JS, Flynn SE, Norman DJ, O'Connell SM, Gukovsky I, Carriere C, Ryan AK, Miller AP, Zuo L, Gleiberman AS, Andersen B, Beamer WG, Rosenfeld MG (1996) Pituitary lineage determination by the Prophet of Pit-1 homeodomain factor defective in Ames dwarfism. Nature 384:327–333

Suh YH, Kim WH, Moon C, Hong YH, Eun SY, Lim JH, Choi JS, Song J, Jung MH (2005) Ectopic expression of neuronatin potentiates adipogenesis through enhanced phosphorylation of cAMP-response element-binding protein in 3T3-L1 cells. Biochem Biophys Res Commun 337:481–489

Susa T, Kato T, Kato Y (2008) Reproducible transfection in the presence of carrier DNA using FuGENE6 and Lipofectamine 2000. Mol Biol Rep 35:313–319

Susa T, Ishikawa A, Kato T, Nakayama M, Kato Y (2009) Molecular cloning of paired related homeobox 2 (Prx2) as a novel pituitary transcription factor. J Reprod Dev 55:502–511

Susa T, Kato T, Yoshida S, Yako M, Higuchi M, Kato Y (2012) Paired-related homeodomain proteins Prx1 and Prx2 are expressed in embryonic pituitary stem/progenitor cells and may be involved in the early stage of pituitary differentiation. J Neuroendocrinol 24:1201–1212

Usui H, Ichikawa T, Miyazaki Y, Nagai S, Kumanishi T (1996) Isolation of cDNA clones of the rat mRNAs expressed preferentially in the prenatal stages of brain development. Brain Res Dev Brain Res 97:185–193

Wang L, Li W, Yang Y, Hu Y, Gu Y, Shu Y, Sun Y, Wu X, Shen Y, Xu Q (2014) High expression of sarcoplasmic/endoplasmic reticulum Ca(2+)-ATPase 2b blocks cell differentiation in human liposarcoma cells. Life Sci 99:37–43

Wijnholds J, Chowdhury K, Wehr R, Gruss P (1995) Segment-specific expression of the neuronatin gene during early hindbrain development. Dev Biol 171:73–84

Wu W, Cogan JD, Pfaffle RW, Dasen JS, Frisch H, O'Connell SM, Flynn SE, Brown MR, Mullis PE, Parks JS, Phillips JA 3rd, Rosenfeld MG (1998) Mutations in PROP1 cause familial combined pituitary hormone deficiency. Nat Genet 18:147–149

Yoshida S, Kato T, Susa T, Cai L-Y, Nakayama M, Kato Y (2009) PROP1 coexists with SOX2 and induces PIT1-commitment cells. Biochem Biophys Res Commun 385:11–15

Yoshida S, Kato T, Yako H, Susa T, Cai L-Y, Osuna M, Inoue K, Kato Y (2011) Significant quantitative and qualitative transition in pituitary stem/progenitor cells occurs during the postnatal development of the rat anterior pituitary. J Neuroendocrinol 23:933–943

Yoshida S, Kato T, Higuchi M, Yako H, Chen M, Kanno N, Ueharu H, Kato Y (2013) Rapid transition of NESTIN-expressing dividing cells from PROP1-positive to PIT1-positive advances prenatal pituitary development. J Neuroendocrinol 25:779–791

Yoshida S, Kato T, Chen M, Higuchi M, Ueharu H, Nishimura N, Kato Y (2015) Localization of a juxtacrine factor ephrin-B2 in the pituitary stem/progenitor cell niches throughout life. Cell Tissue Res 359:755–766

Zhu X, Gleiberman AS, Rosenfeld MG (2007) Molecular physiology of pituitary development: signaling and transcriptional networks. Physiol Rev 87:933–963